

Classification of Corn Seed Quality Using Convolutional Neural Network with Region Proposal and Data Augmentation

Budi Dwi Satoto¹, Rima Tri Wahyuningrum², Bain Khusnul Khotimah³

¹Information System Universitas Trunojoyo Madura, Bangkalan, Jawa Timur 69162, Indonesia

^{2,3}Informatics Engineering Universitas Trunojoyo Madura, Bangkalan, Jawa Timur 69162, Indonesia

ARTICLE INFO

Article history:

Received April 12, 2023

Revised May 19, 2023

Published May 22, 2023

Keywords:

Corn seed;
Deep learning;
Convolutional neural network;
Region proposal;
Convex Hull;
Data augmentation

ABSTRACT

Corn is a commodity in agriculture and essential to human food and animal feed. All components of corn can be utilized and accommodated for the benefit of humans. One of the supporting components is the quality of corn seeds, where specific sources have physiological properties to survive. The problem is how to get information on the quality of corn seeds at agricultural locations and get information through direct visual observations. This research tries to find a solution for classifying corn kernels with high accuracy using a convolutional neural network. It is because in-depth training is used in deep learning. The problem with convolutional neural networks is that the training process takes a long time, depending on the number of layers in the architecture. The research contribution is adding Convex Hull. This method looks for edge points on an object and forms a polygon that encloses that point. It helps increase focus on the convolution multiplication process by removing images on the background. The 34-layer architecture maintains feature maps and uses dropout layers to save computation time. The dataset used is primary data. There are six classes, AR21, Pioner_P35, BISI_18, NK212, Pertiwi, and Betras1—data augmentation techniques to overcome data limitations so that overfitting does not occur. The results of the classification of corn kernels obtained a model with an average accuracy of 99.33%, 99.33% precision, 99.33% recall, and 99.36% F-1 score. The computational training time to obtain the model was 2 minutes 30 seconds. The average error value for MSE is 0.0125, RMSE is 0.118, and MAE is 0.0108. The experimental data testing process has an accuracy ranging from 77% -99%. In conclusion, using the proposal area can improve accuracy by about 0.3% because the focused object helps the convolution process.

This work is licensed under a [Creative Commons Attribution-Share Alike 4.0](https://creativecommons.org/licenses/by-sa/4.0/)



Corresponding Author:

Budi Dwi Satoto, Universitas Trunojoyo Madura, Telang Street PO.BOX 2 Kamal, Bangkalan 69162, Indonesia

Email: budids@trunojoyo.ac.id

1. INTRODUCTION

Seed quality is essential in maize production as it directly impacts the final yield and productivity of the crop. High-quality seeds tend to have better resistance to plant diseases, including against pathogen attacks, and reduce the risk of yield losses due to infection. High-quality seeds can produce vigorous, healthy plants, overgrow, and potentially provide higher production values. In addition, good sources ensure consistency in growth and crop yields. Adaptability to environmental conditions means these seeds can better survive and produce good crops in various soil, weather, and climatic conditions. Farmers can maximize the use of fertilizers and water more efficiently. Plants derived from high-quality seeds can absorb nutrients and water better, reducing waste and increasing farming efficiency. By choosing high-quality sources, farmers can increase their chances of success in maize production, reduce the risk of losses due to disease or unfavorable environmental conditions, and increase the productivity and profitability of their farming business [1][2].

The research background on the effect of corn seed quality on plant resistance is research that examines how the quality of corn seed can affect the ability of corn plants to withstand environmental stresses such as drought, pest attack, and disease. This research will be conducted on the quality of corn seeds, including size, weight, and germination rate. Next, the seeds will be planted in the field, and their growth will be monitored for several weeks or months. During monitoring, it was noted whether plants grown from seeds of lower quality were more resistant to environmental stress and had higher productivity compared to plants grown from seeds of less quality. In addition, research will also examine whether there are differences in plant responses to different types of environmental stressors. The results of this research can help corn seed farmers and producers choose seeds of higher quality and resistant to environmental stress, thereby increasing the production and sustainability of corn farming [3].

Research on the quality of corn seeds can be observed using a camera with artificial intelligence (AI). This method, known as computer vision, allows taking pictures of corn seeds and automatically analyzing their quality using AI algorithms. In this case, the camera will take an image of the corn seed and then use AI technology to identify the seed quality based on features such as size, shape, and sprouts. After that, the AI algorithm will perform an analysis to classify the corn seeds into different quality groups. This method has several advantages, such as the ability to perform analysis quickly and accurately, reducing the need for human labor in selecting seeds, and increasing the efficiency of corn seed production. AI technology in this research also requires complex data processing and precise parameter settings to ensure accurate results [4].

The related work from the past research is the investigation to classify various types of corn seeds using a machine learning approach. Dataset Corn seeds included six varieties first Kashmiri Makkai, second third Pioneer P-1429, fourth Desi Makkai, fifth ICI 339Sygenta ST-6142, and sixth Neelam Makkai. Image capture is carried out in a natural environment without complicated devices. The feature dataset combines the histogram, texture, and spectral features of the data obtained and converted into aggregated data. Fifty-five hybrid features were obtained for each corn seed image in each non-overlapping area of interest (ROI). Bayesian, Random Forest, LogitBoost, and Multilayer Perceptron methods were used to build a model with K-Fold = 10 for nine classes obtained using Best First search in a correlation-based feature selection technique. Comparative analysis of four ML classifiers, MLP yielded excellent classification accuracy (98.93%) at the pixel size ROI (150×150). The MLP accuracy values for six varieties of corn seeds are 99.8%, 97%, 98.5%, 98.6%, and 99.9% [5].

Combined hyperspectral images processed using a deep convolutional neural network (DCNN) are used to classify four varieties of corn seeds. The goal is to get the purity of corn seed varieties because the rice quality affects the growth and development of seed yields. First, the averaged spectrum of the seed region in hyperspectral images of the endosperm side over the 450–979 nm wavelength range was extracted. Second, the test accuracy rate is 94.4%, and the validation accuracy rate is 93.3%. It outperforms the KNN and SVM models. Compared to the performance of the three models, which include the K Nearest Neighbor (KNN) Vector Support Machine (SVM) and DCNN, the DCNN Model has a training accuracy rate close to 100%. The DCNN model also performs best in the evaluation index. Classification process performance level can be improved effectively. DCNN can be adopted to analyze spectral data to classify maize seed varieties. It is because the values for specificity, sensitivity, and precision of the visual classification map show pretty good results [6].

Research on the Automatic Classification of Corn Seed Varieties using deep learning shows that using CNN shows a better classification accuracy of maize seed varieties than models based only on superficial characteristics using machine learning. Machine learning methods include Artificial Neural Network, Cubic Support Vector Machine, Weighted K-Nearest-Neighbor, Quadratic SVM, Bagged Tree, Enhanced Tree, and Linear Discriminant Analysis (LDA) methods. Research shows that intelligent classification of corn seed varieties using CNN-ANN is the most efficient method. The model trained with features extracted from 2250 test samples gets the best performance, as it takes 26.8 seconds of test time with 98.1% classification accuracy, 98.2% precision, 98.1% recall, and 98.1 F1 % score % [7].

From the literature review above, the authors try to develop a more efficient and accurate method for identifying and classifying corn seed varieties using computer vision and a convolutional neural network. This research aims to overcome the limitations of the previous approach by increasing the focus on the object region of the corn seed using the convex hull algorithm. The gap with previous research is that previous research still uses form identification that requires ground truth or experts. For CNN research, the resulting accuracy is quite good, but the drawback is the relatively high computational time needed for the training process. The first research contribution is to increase the focus area of the corn seed object so that it is more precise using the convex Hull algorithm, and the second is to use data augmentation techniques to overcome data limitations so that overfitting does not occur. In addition, the use of custom layers helps save computation time. It is hoped

that better accuracy will be obtained at the right time when the training process is carried out, and stability will be maintained.

2. METHODS

Regarding the limitations of visual observation methods to classify corn seed varieties, the researchers helped highlight the need for a better approach, such as a method based on the Convolutional neural network. The process begins with data acquisition, carried out directly at shops around the corn fields. The specific criteria for choosing a farm shop include seed quality, high clarity, reasonable seed sufficiency, free from disease and contamination, having a business permit and being recommended by the local agriculture department, having certification and authenticity of seeds, having a reputation and experience, have customer service and of course competitive price.

The data acquisition process is carried out in different places with cameras from four district areas in Madura, Indonesia. Before the CNN process, it is necessary to do preprocessing to equalize the size of the image, and the proposed method is the convex hull proposal [8][9]. This research begins by defining the general description shown in Fig. 1. The figure explains the process starting from preprocessing data collection, equalizing size, and bit depth, and doing region proposals to get the image boundaries of the object to be observed. The region proposal helps overcome the limitations of the previous method by increasing the focus on the object region of the corn kernel [10][11].

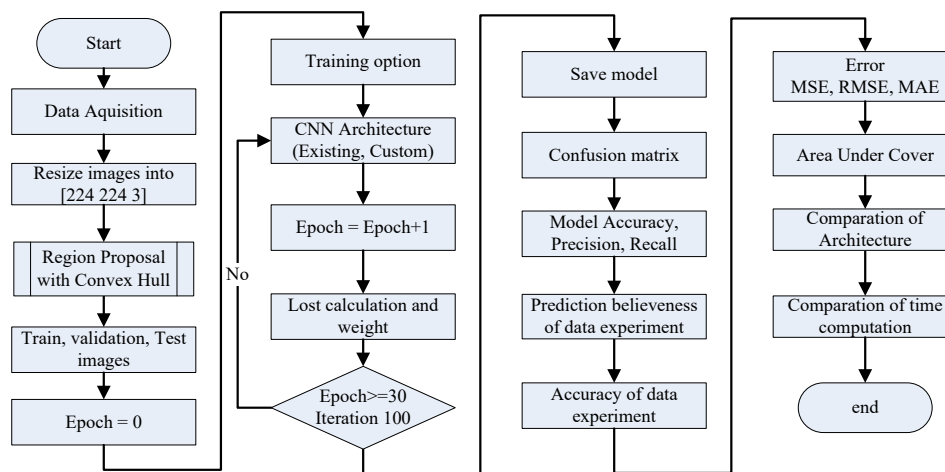


Fig. 1. Research Methods

The data is divided into training data, validation, and testing before being processed using a Convolutional neural network (CNN). The data is divided into training, validation, and test data before processing using a Convolutional neural network. The rules for dividing the data used are training: testing = 80%: 20% testing of the total data. In comparison, the validation data is taken in the 20-80% range of the training data. Besides, experimental or new test data are images not found in training and testing [12][13].

Data augmentation is used to overcome the limited data and balance the image data per class. In the training process, a model is generated. The model here is formed from the results of neural network training based on the training data provided. The model is stored in the memory array to remember the weight and rules used during training. The selection of training options includes setting mini-batch parameters, learning rate, number of epochs, iterations, etc. All the features are used in the CNN feature map process because the convolution process examines all the pixels. The architectures currently used include alexnet, googlenet, VGG-19, resnet-50, and densenet-201. The confusion matrix determines the level of accuracy of the resulting model. Then the prediction of experimental data is carried out to become the accuracy of the belief. In the final stage, an evaluation is carried out to get performance [14][15].

2.1. Explanation of dataset

There are six classes used to be trained. The data takes from cropland, and each type has shown in Fig. 2. The data used is primary data. Due to limited secondary data on the internet, there is no dataset for this corn seed for the Asian region. Available data is from the Indian territory. The data is taken from four districts in the Madura region, Indonesia. Each class has 50 images, so the total data is 300.

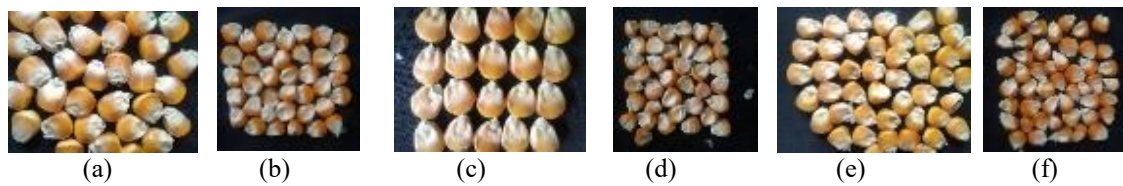


Fig. 2. Types of corn seed (a) AR21, (b) Pioner_P35, (c) BISI_18, (d) NK212 (e) Pertiwi, (f) Betras1

Image taken from Xiaomi camera Redmi Note 8 with size 1200×1600 pixels, resolution with a depth of 72 dpi. Because of the limited data, data augmentation techniques use scale, rotation, flip, and reflection. The goal is that in the training process, there is no overfitting. The definition of each class is as follows:

a. AR_21

The Pioneer P21 Hybrid Corn Seed is a single cross hybrid with a yield potential of ± 13.3 tons/ha dry-shelled. The specifications are full and small cob, guaranteeing high yield, disease resistance, leaf rust tolerance, and drought resistance [16].

b. Betras_1

A domestic innovation product with solid stems, large cobs, high yields of more than 80%, mildew resistant, leaf rust resistant, and leaf blight resistant [17].

c. BISI_184

Indonesian farmers' mainstay varieties have high productivity, have excellent resistance and tolerance to pests and diseases. It is suitable for planting in irrigated and rainfed rice fields [16].

d. NK212

NK 212 is a hybrid corn seed with a tall tree stature but with broader leaves and disease resistance. These seeds resist downy mildew and stem rot, strengthening the tree. Harvest time is quicker, around 100 days, and average yields reach more than 6 tonnes per hectare [17].

e. Pertiwi

PERTIWI hybrid corn seeds are super hybrid seeds produced from crosses of superior, mildew-resistant corn varieties. Pertiwi Corn 3 has a distinctive character: the cob looks big and fat. The advantage of Pertiwi-3 corn is its resistance to fluff [18].

f. Pioneer_P35

Hybrid corn seed type P35 Banteng is the newest variety, with a vital source and bold against downy mildew. Farmers can harvest results quickly because they have about 100 days after planting. The seeds are bright red, the quality of the shell is excellent, the cobs are easy to pick, and the moisture content is low. The cob size is large and guarantees a yield of ± 12.1 tons/ha [19].

2.2. Convex Hull

The convex hull is a closed set and is convex from all points in space. In a two-dimensional plane, a convex hull is defined as a minor polygon shape that can cover all topics in that plane. In three dimensions, a convex hull can be defined as the most petite polyhedron shape that can cover all points in that space [20][21]. The orientation of the Convex Hull to find the node is shown in Fig. 3.

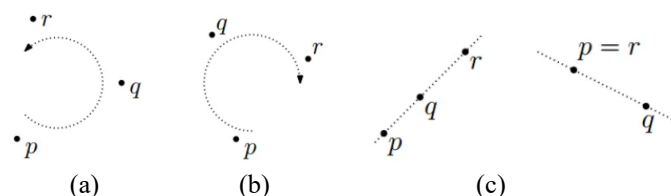


Fig. 3. Convex Hull Orientation (a) $(p,q,r) > 0$, (b) $(p,q,r) < 0$, (c) $(p,q,r) = 0$ (23)

The Convex Hull algorithm will determine whether the points p , q , and r turn left or right using the determinant. Intuitively, the convex hull can be considered the outer shell of the set of points within it. This concept has many applications in computational geometry, data analysis, image processing, and algorithm

design. For example, a convex hull can be used to find the boundaries of objects in a digital image or to solve optimization problems involving sets of points in space [22][23]. The flowchart is shown in Fig. 4.

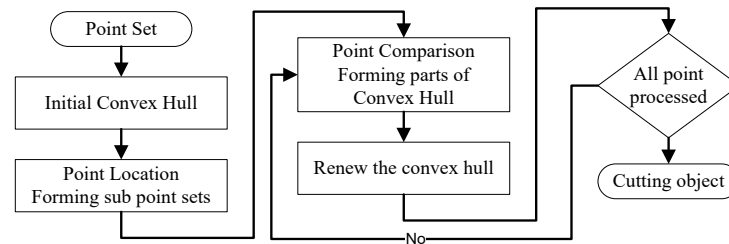


Fig. 4. Convex Hull Flowchart

The convex hull process begins by determining the starting point set of pixels. These points can be obtained from geometric coordinates. Sort the issues by x or y coordinates ascending or descending. Choose the case with the lowest coordinates as the starting point on the convex hull. From the starting point, iterate at another point clockwise or counterclockwise to form a convex hull. At each end visited, check whether the moment is on the left or right side of the line connecting the previous point to the current issue. If the matter is on the left side, it is a point that can potentially become part of the convex hull. Continue iterating until you return to the starting point. When it returns to the starting point, the convex hull is complete. If issues are not included in the convex hull, but inside the formed convex shell, these points can be deleted or considered outliers [24][9].

2.3. Convolutional neural network

This method is one of the Deep Learning algorithms used to process image data. Existing architectures such as alexnet, googlenet, vgg, densenet, and squeezeNet were used in the scenarios conducted. The proposed method uses a Custom 34 layer to save computation time, while the structure is shown in Fig. 5.

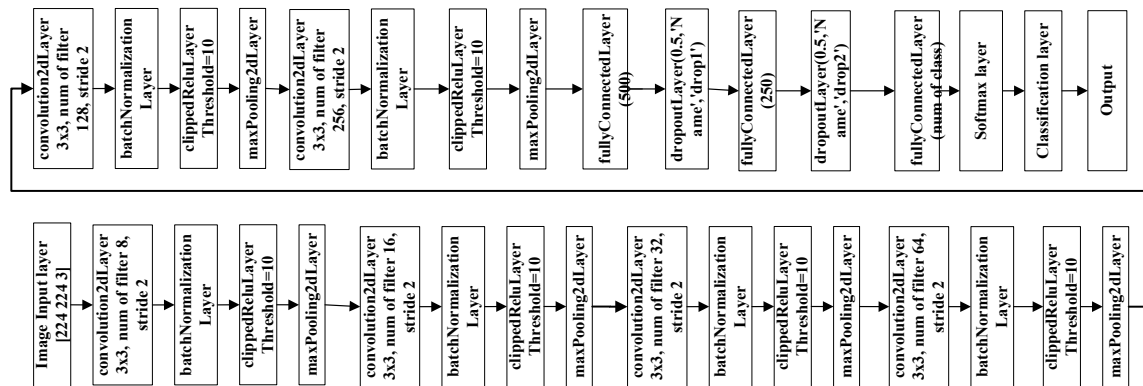


Fig. 5. Purpose CNN Custom Layer architecture 34 layer

The Convolution Layer consists of multiple convolution filters (kernels) that are shifted incrementally across the input image. Each filter takes local information from the input and calculates the convolution operation with that filter. The result of each filter shift will produce one feature map. Each feature map represents the level of presence of specific features in the input image. Activation Layers such as ReLU handling non-linearity. The activated Feature maps pass through the max pooling layer to reduce the spatial dimension of the feature maps. Each non-overlapping area is maintained in the smaller feature maps. This process helps reduce complexity in computations. The Convolution and Activation Layers can be repeated several times to refine the convolution process [25]. Each iteration produces increasingly complex feature maps with more abstract representations of features. In the classification process, the vector image is converted into a single feature vector and given to the fully connected layers, whose job is to process this feature and produce output in the form of class probability values. At the end of the layer, the softmax activation function generates class probabilities. Furthermore, the output model can compare new image patterns [26][27]. Detailed confirmation of each layer can be defined as follows:

a. Convolution layer

Convolution is a mathematical term that repeatedly multiplies the input function by the filter kernel [28][29]. The output of the convolution process is shown in (1).

$$O_w = \frac{W - F_w + 2P}{s_w} + 1 \text{ and } O_h = \frac{H - F_h + 2P}{s_h} + 1 \quad (1)$$

Where O_w =Output width, O_h =Output height, W =Width, F_w =Filter width, F_h =Filter height, P =Polling, s =stride. The filter on this layer is a 2-dimensional array that can be 5×5 , 3×3 , or 1×1 in size width. The feature map used in the activation layer comes from the convolution process of the input image with the kernel filter at this Layer [30][31].

b. Activation Layer

The activation function changes the values in the feature map in a specific range according to the activation function used [32][33].

$$ReLU(x) = f(x) = \begin{cases} x, & \text{if } x \geq 0 \\ 0, & \text{others} \end{cases} \quad (2)$$

Where x = the input value of a pixel, $f(x)$ =function of ReLU. The importance of ReLU will be zero if the input of x is less than zero, and the output will be the value of x if the input value of x is more or equal to zero [34][35].

c. Polling Layer

The pooling layer receives input from the activation layer and reduces the parameters [36][37].

$$Pooling\ layer = \left\lfloor \left(\frac{W - F}{S} + 1 \right) \right\rfloor \quad (3)$$

Where W = size of input image, ex $15 \times 15 \times 3$ then $W=15$, F =Filter size, ex 2×2 then F value=2, S =Stride, ex $S=2$. Therefore, the output has a spatial size $(15 - 2)/2 + 1 = [7 \times 7 \times 10]$. Polling, also known as subsampling or down sampling, reduces the dimensions of the feature map without losing important information [38][39].

d. Fully Connected Layer

Each neuron in the fully connected layer receives input from each neuron in the previous layer. Each intake is associated with an associated weight. This weight will modify the contribution of each piece of information to the activation of neurons in the fully connected Layer [40][41].

2.3. Data Augmentation

It is one technique to manipulate data without losing the essence or essence of the original file. Four kernels include scale, rotation, shears, and reflection [42].

$$A_1 = \begin{bmatrix} C_x & 0 & 0 \\ 0 & C_y & 0 \\ 0 & 0 & 1 \end{bmatrix}; A_2 = \begin{bmatrix} \cos(q) & \sin(q) & 0 \\ -\sin(q) & \cos(q) & 0 \\ 0 & 0 & 1 \end{bmatrix}; A_3 = \begin{bmatrix} 1 & s_v & 0 \\ 0 & 1 & 0 \\ 0 & 0 & 1 \end{bmatrix}; A_4 = \begin{bmatrix} 1 & 0 & 0 \\ s_h & 1 & 0 \\ 0 & 0 & 1 \end{bmatrix} \quad (4)$$

Where A_1 = Matrix kernel for scaling, A_2 = Matrix kernel for rotation, A_3 = Matrix kernel for shears vertical, A_4 = Matrix kernel for shears horizontal, C_x =Scaling horizontal, C_y =Scaling horizontal, q =angle degree, s_v =value shears vertical, s_h = value shears horizontal [43][44].

2.4. Confusion Matrix

In the confusion matrix, each row represents the actual class (ground truth), while each column represents the class predicted by the model. Each entry in the matrix describes the number of data instances classified into each category based on predictions and actual values [45][46].

$$Accuracy = \frac{TP + TN}{TP + TN + FP + FN} \quad (5)$$

Where True Positive (TP) is The actual value, as well as the predicted value, are the same, False Negative (FN) is the actual value is positive, but the prediction is pessimistic, False Positive (FP) is the actual value is negative. The prediction is optimistic, True Negative (TN) is the actual positive and predicted values are negative [47][48].

2.5. Error Calculation

The error of the prediction process for the next model is calculated using Mean Square Error (*MSE*) to calculate the mean squared error, Root Mean square Error (*RMSE*) calculates the root of the mean squared error, and Mean Absolute Error (*MAE*) estimates the error of the absolute difference in price [49][50].

$$MSE = \frac{1}{n} \sum_{i=1}^n (y_i - \hat{y}_i)^2 ; RMSE = \sqrt{\frac{1}{N_d} \sum_{k=1}^{N_d} (y_k - \hat{y}_k)^2} ; MAE = \frac{1}{n} \sum_{j=1}^n |y_j - \hat{y}_j| \quad (6)$$

Where n =number of data samples, i, j, k = indexing, y_i, y_k, y_j =actual label, and $\hat{y}_i, \hat{y}_k, \hat{y}_j$ = prediction label [51][52]. Meanwhile, the value is smaller for MAE because it is taken from the absolute price difference. [53][54].

2.6. Hardware Requirement

The hardware used to process the data in this research is an HP laptop (Hewlett Packard) with an 8th generation Core i-7 processor, 8GB RAM, Graphics Processing Unit Nvidia Ge Force GTX1050 with 4GB VRAM, 256GB SSD, 1GB hard drive, and Windows10. The use of the GPU enables efficient parallel processing of larger batches of data, reducing the time required to train the model on the entire dataset [55][56].

3. RESULTS AND DISCUSSION

This section presents the results of this current research, including preprocessing, region proposal, training process, data augmentation, prediction, error calculation, and comparison.

3.1. Preprocessing Resize Image

The initial stage is to equalize all images to have a size of 224x224x3. The photos in the dataset are taken from different places with different cameras. The same instruction is the camera distance one meter from the object and has a background velvet cloth. The result after resizing is shown in Fig. 6.



Fig. 6. Image input after Resize to process

Interpolation techniques for resizing images include bilinear interpolation, bicubic interpolation, nearest neighbor interpolation, and Lanczos interpolation. This process is also required to use all images used in the feature maps stage and the training, validation, and testing folders during the convolution multiplication process with the kernel or filter. The next step is to get the region image for the corn seed.

3.2. Region Proposal

Furthermore, after all the images have the same size and match the CNN input layer, a convex hull process is carried out to get the foreground image object and remove the background. Convex Hull works to get the image edges of an object so that it cuts the edges of things that are not needed. It is intended that the convolution process focuses on the image being observed by making the background object only white or black. If an image contains irregular objects, a convex hull can produce a polygon that surrounds the thing to separate it from the background. Convex Hull takes a collection of points on the object to be processed. Form a set of issues that form the smallest convex polygon that can cover all these points. Use the resulting convex polygons as a basic shape for further analysis, such as object recognition or image segmentation. It shows in Fig. 7.

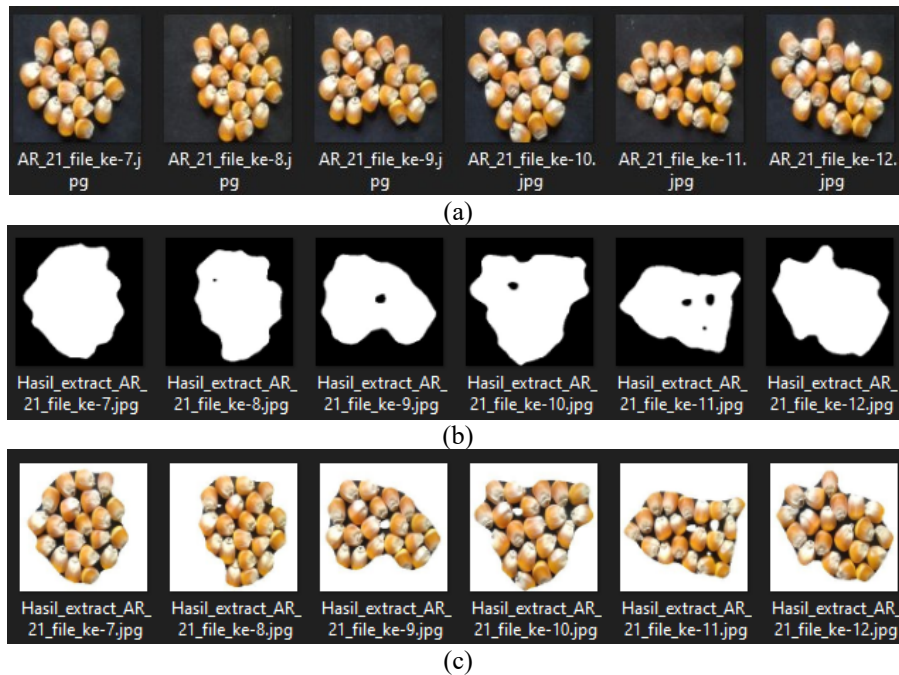


Fig. 7. Convex Hull (a) original image (b) segmented image (c) Cropping image

The proposal region is obtained from the search calculation for the convex hull value in finding the edge value of the object. After getting this value, the pixel nodes are cut so that they can be used to separate the foreground from the background. Convex Hull's effectiveness can be measured by calculating computational time or comparison with the actual ground truth. Still, in this research, the success of the Convex Hull can be seen from the accuracy of the resulting CNN. The anchors can be used by taking them from the output of feature maps, but there are also problems with computation time.

3.3. Training Process

Before starting the CNN training process, several parameters must be determined first: learning rate = 3e-4, minibatch size = 5, iterations per epoch = 35, and max epoch 30. There are training optimization menu options such as ADAM (adaptive moment), SGDM (gradient descent), and rmsprop (root mean square prop). The training process with optimization is shown in Fig. 8.

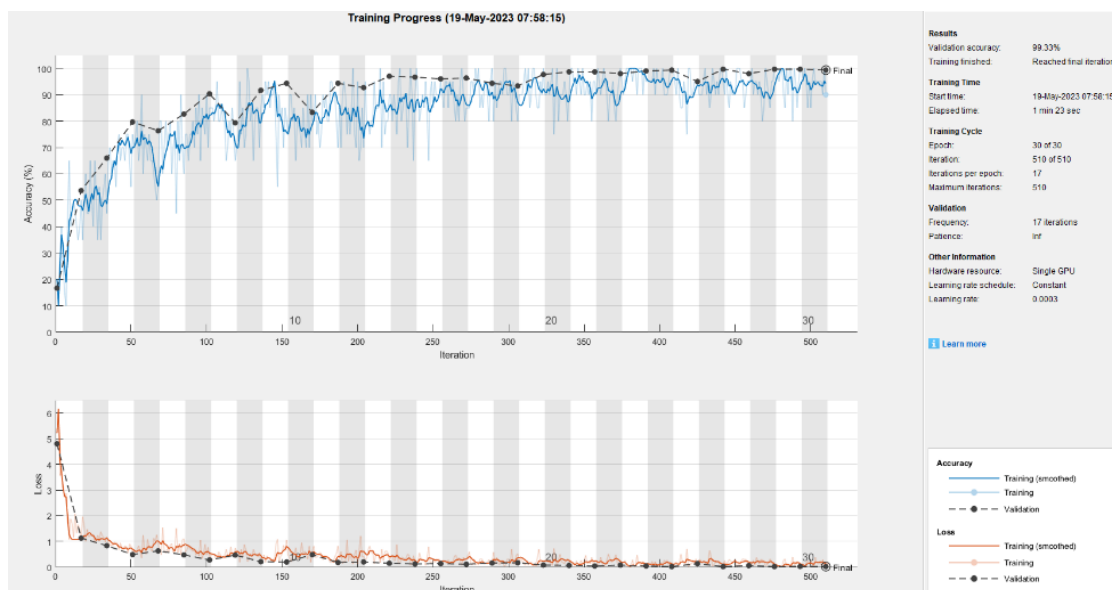


Fig. 8. Training Process

3.4. Data Augmentation

The weakness of primary data is that the number of datasets is limited, so training requires more image variations. It can be done using augmentation, including scale, rotation, and shears shown in Fig. 9. Augmentation adds variety to the data and overcomes the limited amount of data so that the dataset used for training to obtain the model does not experience overfitting.

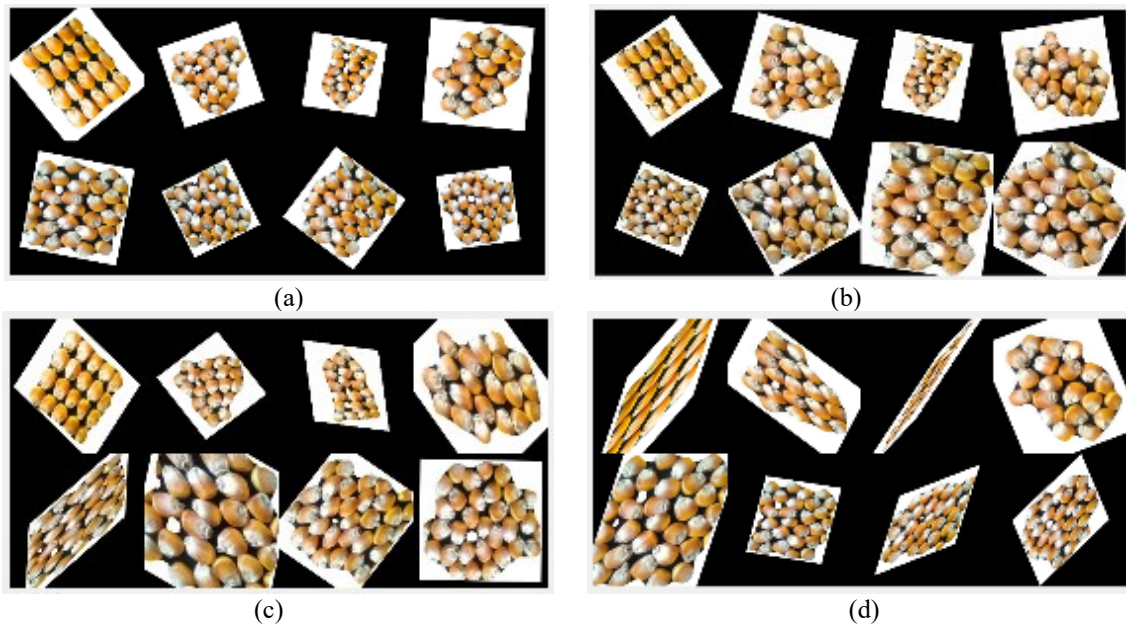


Fig. 9. Augmentation Data (a) Scaling (b) Rotation (c) Shears (d) Reflection

3.5. Confusion Matrix

This stage is to explain the classification process errors on CNN. Several files enter the wrong class due to the level of similarity that does not meet. Errors in the confusion matrix process indicate the performance of the model. Fig. 10 shows the classification error that occurred in the classification process using CNN.

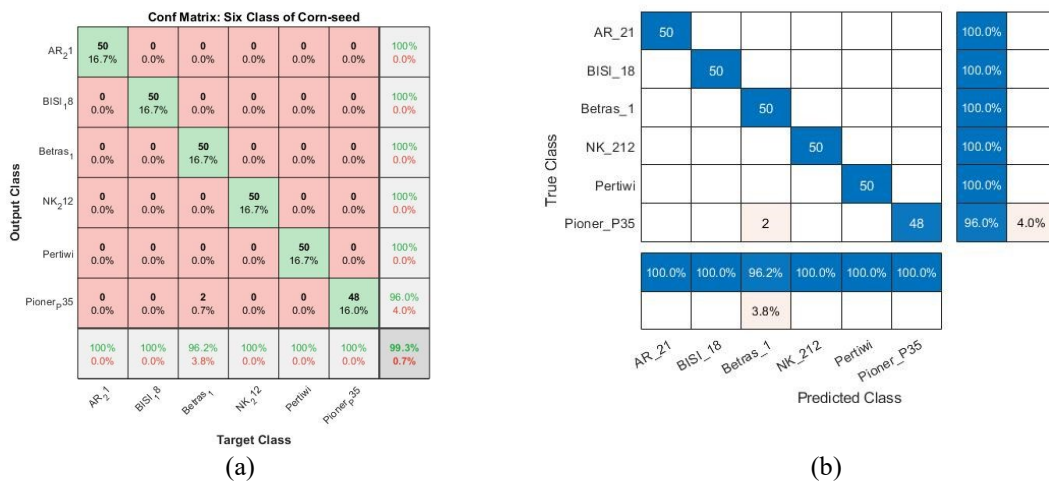


Fig. 10. Confusion Matrix (a) Target (b) Predicted

From around 50 training data per class or 300 total data from six categories, two files for Pioneer_P35 class are classified into Betras_1. The two image files have similarities with other courses, so misclassification occurs. The model accuracy of the training process is 99.33%, and these results are then used to predict the test data to obtain the belief accuracy.

3.6. Prediction

the prediction stage uses to get the confidence value of the test data. The trial was carried out on eight datasets files, and the average results were quite good, above 90%. At this stage, a discussion of the process is carried out from the beginning.

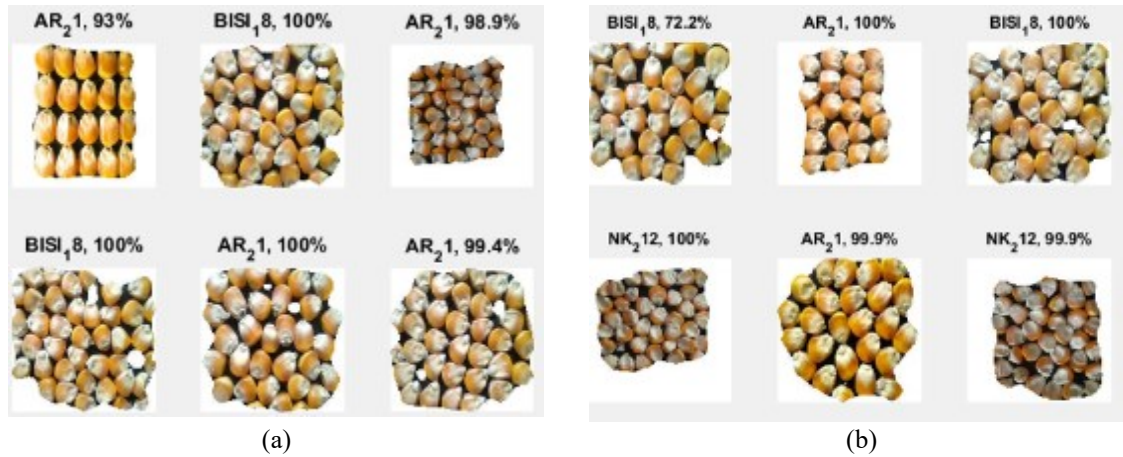


Fig. 11. Result Prediction (a) Believeness 01 (b) Believeness 02

In the first trial shown in Fig. 11.a, there are two images with confidence in the classification results of 93%, 98.9%, and 99.4%. Fig. 11.b shows the results of the prediction process confidence—the confidence interval for testing the model using data ranges from 72.2% -100%. If the training model accuracy results are good, then the prediction will also get a good range of confidence accuracy.

3.7. Error Comparison

Several scenarios were used to test the reliability of the system created, including by comparing the accuracy of the existing architecture, Alexnet, Google, and VGG, with the proposed method. The choice of training optimization, namely Adam (adaptive moment estimation), sgd (Stochastic gradient descent), and rmsprop (Root Mean Square Propagation), also determines the results of the training process. Comparison between the architecture shown in Fig. 12.

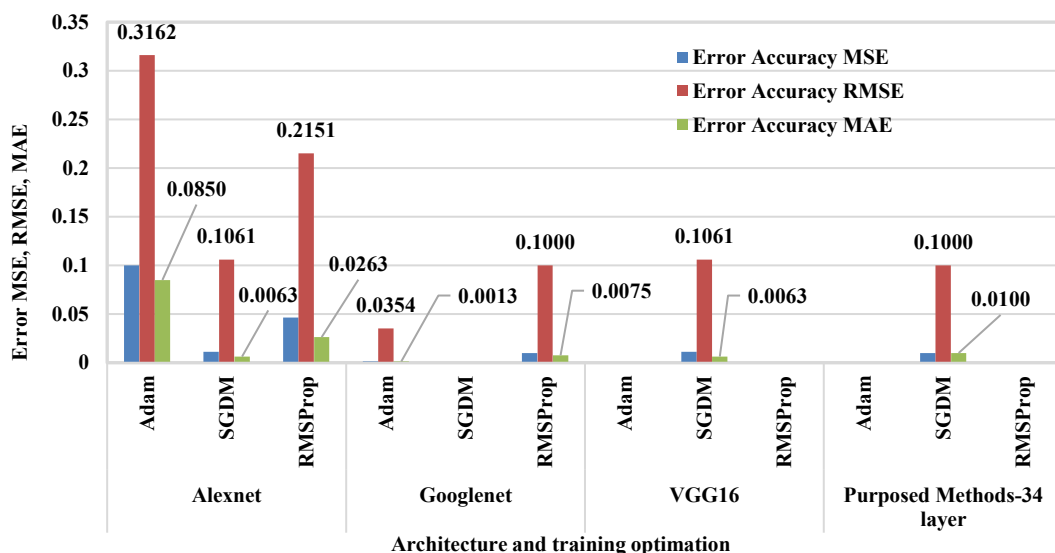


Fig. 12. Comparison of classification errors

The graph shows that the proposed method has better accuracy and time than other architectures tested in the scenarios. In using Adam optimization and rmsprop, there is no misclassification. However, when using

sgdm, the optimal MSE, RMSE, and MAE values are obtained. A comparison of accuracy and training time is shown in Table 1.

Table 1. Comparison of accuracy and training time

| Models | No.of layer | Training | |
|-------------------|-------------|----------|---------------|
| | | Accuracy | Time (minute) |
| Alexnet | 25 | 99.50% | 4.50 |
| Googlenet | 144 | 99.75% | 10.03 |
| VGG19 | 47 | 100.00% | 45.82 |
| Resnet50 | 177 | 99.88% | 28.34 |
| DenseNet201 | 709 | 100.00% | 348.20 |
| SqueezeNet | 68 | 99.50% | 5.82 |
| Purposed methods | 34 | 99.00% | 2.52 |
| Purposed methods2 | 18 | 99.33% | 2.05 |

Meanwhile in Fig. 13 shows a comparison of the number of layers, training computation time and model accuracy. The scenario results show that when using a large number of layers, the training time increases, but for a small number of layers it is necessary to pay attention to the level of stability or not to experience overfitting. So, the exact requirement is the minimum training time but can produce the desired optimum accuracy

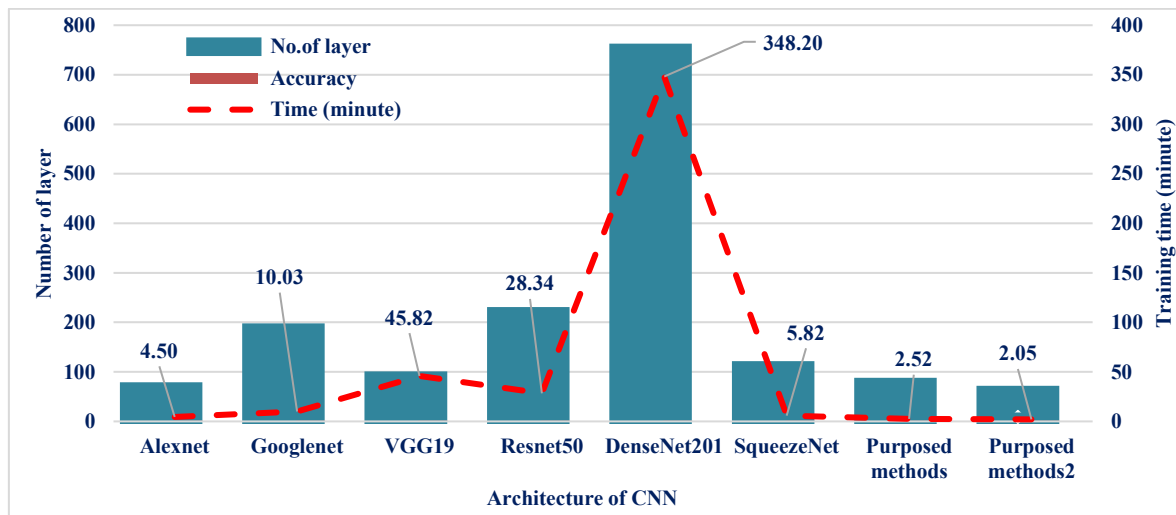


Fig. 13. Comparison number of layers vs. time computation

The graph in Fig. 13 compares the number of layers in each architecture to the computational time required to train the object. In the 34 layers, the best time is obtained because, in this architecture, the stability of the training process has been received with the shortest processing time compared to other architectures in the case of object identification of rice seeds. The time needed to train is around 2.5 minutes.

3.8. Research Comparison

Research on the classification of corn seeds is still limited because the dataset is not yet freely available on the internet, so there are still obstacles to making head-to-head comparisons. In addition, each region or country has its superior corn seed product, which is also related to the soil conditions, climate, and topography of the surrounding environment. Another factor is resistance to pests and diseases. This data can be obtained through the local agricultural service. The scope of coverage area dominates. For example, countries with Asian tropical climates tend to be the same but different from Europe or Africa. Several studies can be used to compare this research regarding the classification of corn seeds, as shown in Table 2.

From the results submitted, not all researchers convey the computational training time but rather indicate the results of the accuracy delivered. The table shows that the results of this research can accurately match the use of Yolo V-5 with a shorter training time.

Table 2. Research comparison

| No | Author | Method | Accuracy | training time (minute) | testing time (s) |
|----|--|-------------------------------|----------|------------------------|------------------|
| 1 | Javanmardi <i>et al.</i> (2021) [7] | CNN-ANN | 98.20% | N/A | 26.8 |
| 2 | Aqib Ali <i>et al.</i> (2020) [5] | Random Forest, Bayesnet, MLP | 94.67% | N/A | 3.81 |
| 3 | Jinghua <i>et al.</i> (2022) [57] | Support Vector machine | 97.92% | N/A | N/A |
| 4 | Xiaoming Li <i>et al.</i> (2019) | Computer vision | 96.67% | N/A | N/A |
| 5 | Jun Zhang <i>et al.</i> (2020) [6] | DCNN | 94.40% | N/A | N/A |
| 6 | Nidhi Kundu <i>et al.</i> (2021) [58] | Yolo V-5 | 99.00% | N/A | N/A |
| 7 | Purposed Method without Convex Hull | Augmented + CNN | 99.00% | 2.5 minute | 0.02 |
| 8 | Purposed Method with Convex Hull Budids <i>et al.</i> (2023) | Augmented + Convex Hull + CNN | 99.33% | 2.05 minute | 0.02 |

4. CONCLUSION

In this research, we have developed a Convolutional Neural Network (CNN) with proposed regions and augmentation techniques to identify maize seeds. The resulting model may differ depending on the data acquisition process and environmental conditions, such as lighting and distance from objects. The implementation of convex Hull in this research sharpens the desired object area, and the augmentation technique overcomes the limited amount of data. The classification results show an average accuracy of 99.33%, 99.33% precision, 99.33% recall, and 99.36% F-1 score. The computational training time to derive the model is about 2 minutes and 30 seconds. The average error value for MSE is 0.0125, RMSE is 0.118, and MAE is 0.0108. Further research that can be done is to increase the amount of primary data. Method improvement can be made by modifying the feature maps layer or improving the Loss function.

Acknowledgments

The authors thank the Directorate General of Higher Education - Ministry of Education, the Faculty of Engineering and Research and Community Development Body of the University of Trunojoyo Madura, Indonesia.

REFERENCES

- [1] A. Ambrose, L. M. Kandpal, M. S. Kim, W.-H. Lee, and B.-K. Cho, "High speed measurement of corn seed viability using hyperspectral imaging," *Infrared Phys. Technol.*, vol. 75, pp. 173–179, 2016, <https://doi.org/10.1016/j.infrared.2015.12.008>.
- [2] E. Prakasa, D. R. Prajitno, A. Nur, K. A. Sulisty, and E. Rachmawati, "Quality Categorisation of Corn (*Zea mays*) Seed using Feature-Based Classifier and Deep Learning on Digital Images," in *2021 International Conference on Innovation and Intelligence for Informatics, Computing, and Technologies (3ICT)*, pp. 498–505, 2021, <https://doi.org/10.1109/3ICT53449.2021.9581464>.
- [3] L. Pang, S. Men, L. Yan, and J. Xiao, "Rapid Vitality Estimation and Prediction of Corn Seeds Based on Spectra and Images Using Deep Learning and Hyperspectral Imaging Techniques," *IEEE Access*, vol. 8, pp. 123026–123036, 2020, <https://doi.org/10.1109/ACCESS.2020.3006495>.
- [4] L. Wang, J. Liu, J. Zhang, J. Wang, and X. Fan, "Corn Seed Defect Detection Based on Watershed Algorithm and Two-Pathway Convolutional Neural Networks," *Front. Plant Sci.*, vol. 13, p. 730190, 2022, <https://doi.org/10.3389/fpls.2022.730190>.
- [5] A. Ali *et al.*, "Machine learning approach for the classification of corn seed using hybrid features," *Int. J. Food Prop.*, vol. 23, no. 1, pp. 1110–1124, 2020, <https://doi.org/10.1080/10942912.2020.1778724>.
- [6] J. Zhang, L. Dai, and F. Cheng, "Corn seed variety classification based on hyperspectral reflectance imaging and deep convolutional neural network," *J. Food Meas. Charact.*, vol. 15, no. 1, pp. 484–494, 2021, <https://doi.org/10.1007/s11694-020-00646-3>.
- [7] S. Javanmardi, S.-H. Miraei Ashtiani, F. J. Verbeek, and A. Martynenko, "Computer-vision classification of corn seed varieties using deep convolutional neural network," *J. Stored Prod. Res.*, vol. 92, p. 101800, 2021, <https://doi.org/10.1016/j.jspr.2021.101800>.
- [8] N. Kieu Linh, P. Thanh An, and T. Van Hoai, "A fast and efficient algorithm for determining the connected orthogonal convex hulls," *Appl. Math. Comput.*, vol. 429, p. 127183, 2022, <https://doi.org/10.1016/j.amc.2022.127183>.
- [9] X. Yuan, S. Chen, H. Zhou, C. Sun, and L. Yuwen, "CHSMOTE: Convex hull-based synthetic minority oversampling technique for alleviating the class imbalance problem," *Inf. Sci. (Ny)*, vol. 623, pp. 324–341, 2023, <https://doi.org/10.1016/j.ins.2022.12.056>.
- [10] Y. Song *et al.*, "Segmentation, Splitting, and Classification of Overlapping Bacteria in Microscope Images for

- Automatic Bacterial Vaginosis Diagnosis,” *IEEE J. Biomed. Heal. Informatics*, vol. 21, no. 4, pp. 1095–1104, 2017, <https://doi.org/10.1109/JBHI.2016.2594239>.
- [11] D. Tom *et al.*, “Reduced memory region based deep Convolutional Neural Network detection,” in *2016 IEEE 6th International Conference on Consumer Electronics - Berlin (ICCE-Berlin)*, pp. 15–19, 2016, <https://doi.org/10.1109/ICCE-Berlin.2016.7684706>.
- [12] M. Koklu, I. Cinar, and Y. S. Taspinar, “Classification of rice varieties with deep learning methods,” *Comput. Electron. Agric.*, vol. 187, p. 106285, 2021, <https://doi.org/10.1016/j.compag.2021.106285>.
- [13] L. Zhang and I. A. Kakadiaris, “Local classifier chains for deep face recognition,” in *2017 IEEE International Joint Conference on Biometrics (IJCB)*, pp. 158–167, 2017, <https://doi.org/10.1109/BTAS.2017.8272694>.
- [14] Y. Permanasari, B. N. Ruchjana, S. Hadi, and J. Rejito, “Innovative Region Convolutional Neural Network Algorithm for Object Identification,” *J. Open Innov. Technol. Mark. Complex.*, vol. 8, no. 4, p. 182, 2022, <https://doi.org/10.3390/joitmc8040182>.
- [15] A. Zeggada, F. Melgani, and Y. Bazi, “A Deep Learning Approach to UAV Image Multilabeling,” *IEEE Geosci. Remote Sens. Lett.*, vol. 14, no. 5, pp. 694–698, 2017, <https://doi.org/10.1109/LGRS.2017.2671922>.
- [16] B. D. Satoto and R. T. Wahyuningrum, “Corn Seed Classification Using Deep Learning as an Effort to Increase Corn Productivity,” in *2021 5th International Conference on Informatics and Computational Sciences (ICICoS)*, pp. 249–254, 2021, <https://doi.org/10.1109/ICICoS53627.2021.9651846>.
- [17] Y. Zhang, C. Lv, D. Wang, W. Mao, and J. Li, “A novel image detection method for internal cracks in corn seeds in an industrial inspection line,” *Comput. Electron. Agric.*, vol. 197, p. 106930, 2022, <https://doi.org/10.1016/j.compag.2022.106930>.
- [18] J. Zhang, Z. Wang, M. Qu, and F. Cheng, “Research on physicochemical properties, microscopic characterization and detection of different freezing-damaged corn seeds,” *Food Chem. X*, vol. 14, p. 100338, 2022, <https://doi.org/10.1016/j.fochx.2022.100338>.
- [19] L. Zhang, Q. Zhang, J. Wu, Y. Liu, L. Yu, and Y. Chen, “Moisture detection of single corn seed based on hyperspectral imaging and deep learning,” *Infrared Phys. Technol.*, vol. 125, p. 104279, 2022, <https://doi.org/10.1016/j.infrared.2022.104279>.
- [20] W. Wang, T. Nie, T. Fu, J. Ren, and L. Jin, “A Novel Method of Aircraft Detection Based on High-Resolution Panchromatic Optical Remote Sensing Images,” *Sensors (Switzerland)*, vol. 17, 2017, <https://doi.org/10.3390/s17051047>.
- [21] Y. Jia *et al.*, “Investigating the geometric structure of neural activation spaces with convex hull approximations,” *Neurocomputing*, vol. 499, pp. 93–105, 2022, <https://doi.org/10.1016/j.neucom.2022.05.019>.
- [22] A. Wong-od, A. Rodtook, S. Rasmequan, and K. Chinnasarn, “Automated segmentation of media-adventitia and lumen from intravascular ultrasound images using non-parametric thresholding,” in *2017 9th International Conference on Knowledge and Smart Technology (KST)*, pp. 220–225, 2017, <https://doi.org/10.1109/KST.2017.7886110>.
- [23] J. Araújo and P. S. M. Arraes, “Hull and geodetic numbers for some classes of oriented graphs,” *Discret. Appl. Math.*, vol. 323, pp. 14–27, 2022, <https://doi.org/10.1016/j.dam.2021.03.016>.
- [24] L. K. Nguyen, C. Song, J. Ryu, P. T. An, N.-D. Hoang, and D.-S. Kim, “QuickhullDisk: A faster convex hull algorithm for disks,” *Appl. Math. Comput.*, vol. 363, p. 124626, 2019, <https://doi.org/10.1016/j.amc.2019.124626>.
- [25] H. I. K. Fathurrahman, A. Ma’arif, and L.-Y. Chin, “The Development of Real-Time Mobile Garbage Detection Using Deep Learning,” *Jurnal Ilmiah Teknik Elektro Komputer dan Informatika (JITEKI)*, vol. 7, pp. 472–478, 2021, <https://doi.org/10.26555/jiteki.v7i3.22295>.
- [26] H. O. Velesaca, R. Mira, P. L. Suárez, C. X. Larrea, and A. D. Sappa, “Deep Learning based Corn Kernel Classification,” in *2020 IEEE/CVF Conference on Computer Vision and Pattern Recognition Workshops (CVPRW)*, pp. 294–302, 2020, <https://doi.org/10.1109/CVPRW50498.2020.00041>.
- [27] Y. Sun, B. Xue, M. Zhang, and G. G. Yen, “Completely Automated CNN Architecture Design Based on Blocks,” *IEEE Trans. Neural Networks Learn. Syst.*, vol. 31, no. 4, pp. 1242–1254, 2020, <https://doi.org/10.1109/TNNLS.2019.2919608>.
- [28] Z. Luo, L. Liu, J. Yin, Y. Li, and Z. Wu, “Deep Learning of Graphs with Ngram Convolutional Neural Networks,” *IEEE Trans. Knowl. Data Eng.*, vol. 29, no. 10, pp. 2125–2139, 2017, <https://doi.org/10.1109/TKDE.2017.2720734>.
- [29] A. Buetti-Dinh *et al.*, “Deep neural networks outperform human expert’s capacity in characterizing bioleaching bacterial biofilm composition,” *Biotechnol. Reports*, vol. 22, p. e00321, 2019, <https://doi.org/10.1016/j.btre.2019.e00321>.
- [30] S. Khaki, H. Pham, Y. Han, A. Kuhl, W. Kent, and L. Wang, “DeepCorn: A semi-supervised deep learning method for high-throughput image-based corn kernel counting and yield estimation,” *Knowledge-Based Syst.*, vol. 218, p. 106874, 2021, <https://doi.org/10.1016/j.knosys.2021.106874>.
- [31] L. Jiao, M. Liang, H. Chen, S. Yang, H. Liu, and X. Cao, “Deep Fully Convolutional Network-Based Spatial Distribution Prediction for Hyperspectral Image Classification,” *IEEE Trans. Geosci. Remote Sens.*, vol. 55, no. 10, pp. 5585–5599, 2017, <https://doi.org/10.1109/TGRS.2017.2710079>.
- [32] C. Bai, L. Huang, X. Pan, J. Zheng, and S. Chen, “Optimization of deep convolutional neural network for large scale image retrieval,” *Neurocomputing*, vol. 303, pp. 60–67, 2018, <https://doi.org/10.1016/j.neucom.2018.04.034>.
- [33] J. Ye, J. Ni, and Y. Yi, “Deep Learning Hierarchical Representations for Image Steganalysis,” *IEEE Trans. Inf. Forensics Secur.*, vol. 12, no. 11, pp. 2545–2557, 2017, <https://doi.org/10.1109/TIFS.2017.2710946>.

- [34] M. Tanaka, "Weighted sigmoid gate unit for an activation function of deep neural network," *Pattern Recognit. Lett.*, vol. 135, pp. 354–359, 2020, <https://doi.org/10.1016/j.patrec.2020.05.017>.
- [35] A. M. Javid, S. Das, M. Skoglund, and S. Chatterjee, "A ReLU Dense Layer to Improve the Performance of Neural Networks," in *ICASSP 2021 - 2021 IEEE International Conference on Acoustics, Speech and Signal Processing (ICASSP)*, pp. 2810–2814, 2021, <https://doi.org/10.1109/ICASSP39728.2021.9414269>.
- [36] P. Singh, P. Raj, and V. P. Namboodiri, "EDS pooling layer," *Image Vis. Comput.*, vol. 98, p. 103923, 2020, <https://doi.org/10.1016/j.imavis.2020.103923>.
- [37] N. Akhtar and U. Ragavendran, "Interpretation of intelligence in CNN-pooling processes: a methodological survey," *Neural Comput. Appl.*, vol. 32, no. 3, pp. 879–898, 2020, <https://doi.org/10.1007/s00521-019-04296-5>.
- [38] X. Liu, J. Centeno, J. Alvarado, and L. Tan, "One Dimensional Convolutional Neural Networks Using Sparse Wavelet Decomposition for Bearing Fault Diagnosis," *IEEE Access*, vol. 10, pp. 86998–87007, 2022, <https://doi.org/10.1109/ACCESS.2022.3199381>.
- [39] M. Dan, C. Guitao, H. Zhihai, and C. Wenming, "Facial expression recognition based on LLENet," in *2016 IEEE International Conference on Bioinformatics and Biomedicine (BIBM)*, pp. 1915–1917, 2016, <https://doi.org/10.1109/BIBM.2016.7822814>.
- [40] J. Guo, W. Wang, Y. Tang, Y. Zhang, and H. Zhuge, "A CNN-Bi LSTM parallel network approach for train travel time prediction," *Knowledge-Based Syst.*, p. 109796, 2022, <https://doi.org/10.1016/j.knosys.2022.109796>.
- [41] B. Ait Skourt, A. El Hassani, and A. Majda, "Mixed-pooling-dropout for convolutional neural network regularization," *J. King Saud Univ. - Comput. Inf. Sci.*, vol. 34, no. 8, pp. 4756–4762, 2022, <https://doi.org/10.1016/j.jksuci.2021.05.001>.
- [42] K. Maharana, S. Mondal, and B. Nemade, "A review: Data pre-processing and data augmentation techniques," *Glob. Transitions Proc.*, vol. 3, no. 1, pp. 91–99, 2022, <https://doi.org/10.1016/j.gltp.2022.04.020>.
- [43] E. A. Hay and R. Parthasarathy, "Performance of convolutional neural networks for identification of bacteria in 3D microscopy datasets," *PLoS Comput. Biol.*, vol. 14, no. 12, pp. e1006628–e1006628, 2018, <https://doi.org/10.1371/journal.pcbi.1006628>.
- [44] S. S. Yadav and S. M. Jadhav, "Deep convolutional neural network based medical image classification for disease diagnosis," *J. Big Data*, vol. 6, no. 1, p. 113, 2019, <https://doi.org/10.1186/s40537-019-0276-2>.
- [45] J. Yang, X. Qu, and M. Chang, "An intelligent singular value diagnostic method for concrete dam deformation monitoring," *Water Sci. Eng.*, vol. 12, no. 3, pp. 205–212, 2019, <https://doi.org/10.1016/j.wse.2019.09.006>.
- [46] I. Markoulidakis, I. Rallis, I. Georgoulas, G. Kopsiaftis, A. Doulamis, and N. Doulamis, "Multiclass Confusion Matrix Reduction Method and Its Application on Net Promoter Score Classification Problem," *Technologies*, vol. 9, no. 4, 2021, <https://doi.org/10.3390/technologies9040081>.
- [47] V. H. Phung and E. J. Rhee, "A High-Accuracy Model Average Ensemble of Convolutional Neural Networks for Classification of Cloud Image Patches on Small Datasets," *Applied Sciences*, vol. 9, no. 21, 2019, <https://doi.org/10.3390/app9214500>.
- [48] P. Purwono and A. Ma'arif, "Linkage Detection of Features that Cause Stroke using Feyn Qlattice Machine Learning Model," *J. Ilm. Tek. Elektro Komput. dan Inform.*, vol. 7, no. 3, pp. 423–432, 2021, <https://doi.org/10.26555/jiteki.v7i3.22237>.
- [49] L. Ying and L. Boqin, "Application of Transfer Learning in Task Recommendation System," *Procedia Eng.*, vol. 174, pp. 518–523, 2017, <https://doi.org/10.1016/j.proeng.2017.01.178>.
- [50] M. Mittal, L. M. Goyal, S. Kaur, I. Kaur, A. Verma, and D. Jude Hemanth, "Deep learning based enhanced tumor segmentation approach for MR brain images," *Appl. Soft Comput.*, vol. 78, pp. 346–354, 2019, <https://doi.org/10.1016/j.asoc.2019.02.036>.
- [51] B. Jonathan, Z. Rahim, A. Barzani, and W. Oktavega, "Evaluation of Mean Absolute Error in Collaborative Filtering for Sparsity Users and Items on Female Daily Network," in *2019 International Conference on Informatics, Multimedia, Cyber and Information System (ICIMCIS)*, pp. 41–44, 2019, <https://doi.org/10.1109/ICIMCIS48181.2019.8985340>.
- [52] E. M. O. Silveira *et al.*, "Object-based random forest modelling of aboveground forest biomass outperforms a pixel-based approach in a heterogeneous and mountain tropical environment," *Int. J. Appl. Earth Obs. Geoinf.*, vol. 78, pp. 175–188, 2019, <https://doi.org/10.1016/j.jag.2019.02.004>.
- [53] P. Kharazmi, M. I. AlJasser, H. Lui, Z. J. Wang, and T. K. Lee, "Automated Detection and Segmentation of Vascular Structures of Skin Lesions Seen in Dermoscopy, With an Application to Basal Cell Carcinoma Classification," *IEEE J. Biomed. Heal. INFORMATICS*, vol. 21, no. 6, pp. 1675–1684, 2017, <https://doi.org/10.1016/j.sysarc.2019.101635>.
- [54] K. P. Smith, A. D. Kang, and J. E. Kirby, "Automated Interpretation of Blood Culture Gram Stains by Use of a Deep Convolutional Neural Network," *J. Clin. Microbiol.*, vol. 56, no. 3, pp. e01521–17, 2018, <https://doi.org/10.1128/JCM.01521-17>.
- [55] S. Mittal and S. Vaishay, "A survey of techniques for optimizing deep learning on GPUs," *J. Syst. Archit.*, vol. 99, p. 101635, 2019, <https://doi.org/10.1016/j.sysarc.2019.101635>.
- [56] B. K. Joardar, J. R. Doppa, P. P. Pande, H. Li, and K. Chakrabarty, "AccuReD: High Accuracy Training of CNNs on ReRAM/GPU Heterogeneous 3-D Architecture," *IEEE Trans. Comput. Des. Integr. Circuits Syst.*, vol. 40, no. 5, pp. 971–984, 2021, <https://doi.org/10.1109/TCAD.2020.3013194>.
- [57] J. Wang, L. Yan, F. Wang, and S. Qi, "SVM Classification Method of Waxy Corn Seeds with Different Vitality Levels Based on Hyperspectral Imaging," *J. Sensors*, vol. 2022, p. 4379317, 2022, <https://doi.org/10.1155/2022/4379317>.

- [58] N. Kundu, G. Rani, and V. Dhaka, *Seeds Classification and Quality Testing Using Deep Learning and YOLO v5*. 2021, <https://doi.org/10.1145/3484824.3484913>.

BIOGRAPHY OF AUTHORS



Budi Dwi Satoto, He is a lecturer in Information Systems at Trunojoyo University. He is originally from Bantul, Yogyakarta, completed his bachelor's degree from the Department of Electrical Engineering, Gadjah Mada University in 2002, his Master's degree from the Department of Informatics, Sepuluh Nopember Institute, Surabaya, in 2010, and completed his doctoral studies at the Faculty of Science and Technology, Airlangga University, Surabaya 2021. His research interests are Information Systems, Computer networking, data mining, deep learning Artificial Intelligence, and Health monitoring systems. Email: budids@gmail.com; budids@trunojoyo.ac.id. Scopus ID: 57201197655, and Orcid ID: <https://orcid.org/0000-0002-1919-0540>.



Rima Tri Wahyuningrum, She is a lecturer in Informatics Engineering at Trunojoyo University. She comes from Madiun, East Java, and completed his bachelor's degree in 2003, her Master's in 2010, and her Doctorate in 2020 from the Department of Electrical Engineering, Surabaya Sepuluh Nopember Institute of Technology. Her research interests are Artificial Intelligence, Image Processing, Medical Informatics, and Health Informatics Multimedia. Email: rimatriwahyuningrum@gmail.com; rimatriwahyuningrum@trunojoyo.ac.id. Scopus ID: 55977023600, and Orcid ID: <https://orcid.org/0000-0003-1760-9341>.



Bain Khusnul Khotimah, She is a lecturer in Informatics Engineering at Trunojoyo University. She is originally from Tulungagung, completed his Bachelor of Electrical Engineering from Brawijaya University in 2003, her Master of Informatics Engineering, November 2010 Institute of Technology, and 2020 Doctorate from the Faculty of Science and Technology, Airlangga University, Surabaya 2020. Her research interests are Information Technology, Data Mining, and Artificial Intelligence. Email: bainkk@gmail.com; bain@trunojoyo.ac.id, and Scopus ID: 57721832200.